

Comparative Analysis of PWM Techniques for Three Level Diode Clamped Voltage Source Inverter

Zulkiflie Bin Ibrahim, Md. Liton Hossain, Ismadi Bin Bugis, Jurifa Mat Lazi, Nurazlin Mohd Yaakop

Department of Power Electronics and Drive, Faculty of Electrical Engineering, Universiti Teknikal Malaysia Melaka, Melaka, Malaysia

Article Info

Article history:

Received Mar 30, 2014

Revised May 22, 2014

Accepted Jun 1, 2014

Keyword:

3LDCI

Multilevel inverter

Pulse width modulation

SPWM

SVPWM

THD

ABSTRACT

Multilevel inverters are increasingly being used in high-power medium voltage industrial drive applications due to their superior performance compared to conventional two-level inverters. There are a number of Pulse width modulation (PWM) techniques applied in recent years. The most widely applied PWM techniques are Sine Pulse Width Modulation (SPWM) and Space Vector Pulse Width Modulation (SVPWM). SPWM is the most simple modulation technique that can realize easily in analog circuit. However, it has some drawbacks such as higher total harmonic distortion (THD), lower effective DC utilization and lower switching frequency. Space vector pulse width modulation (SVPWM) is widely used because of their easier digital realization and better DC bus utilization and lower THD. The complexity is due to the difficulty in determining the reference vector location, on times calculation, and switching states selection. This paper presents a simple SVPWM algorithm for diode clamped three level inverters based on standard two-level SVPWM which can easily determine the location of reference vector, calculate the on-times, the selection of switching states. Three level diode clamped inverter (3LDCI) using space vector modulation technique has been modeled and simulated using MATLAB/SIMULINK and Origin 6.1 with a passive R-L load that can be extended to any level. Simulation results are presented to verify the proposed SVPWM control in terms of THD. The results are compared with conventional sinusoidal pulse width modulation (SPWM) where SVPWM shows better performance than SPWM in terms of THD.

Copyright © 2014 Institute of Advanced Engineering and Science.
All rights reserved.

Corresponding Author:

Zulkiflie Bin Ibrahim,

Associate Professor,

Department of Power Electronics and Drive,

Faculty of Electrical Engineering, Universiti Teknikal Malaysia Melaka,

Hang Tuah Jaya, 76100 Durian Tunggal, Melaka, Malaysia.

Email: drzulkiflie@utem.edu.my

1. INTRODUCTION

Multilevel inverter technology has emerged recently as a very important alternative in the area of high-power medium voltage energy control. Today, it is hard to connect a single power semiconductor switch directly to medium voltage grids. Harmonic distortion is high for conventional inverter. For these reasons, a new family of diode clamped multilevel inverters has emerged as the solution for working with higher voltage levels and lower harmonic distortion [1]. Rodríguez and Lai discussed several multi-level inverter topologies to increase the power delivered to the load and to improve the quality of the voltage [2]. In this paper, a diode clamped three level voltage source inverter is presented. This clamping diode can produce additional voltage level that reduces the harmonic distortion.

A various pulse width modulation (PWM) techniques have been discussed to control the inverter [3]. Among these modulation techniques for a multilevel inverter, SVPWM is the most popular technique due to their unique characteristics such as directly using the control variable, improving DC link voltage utilization, reducing commutation losses and THD, easy DSP implementation and optimization of switching patterns [4], [5]. The space vector diagram consists of six sectors for any level inverter. Each sector contains $(m-1)^2$ triangles where m is the number of levels in which the reference vector can be located within any of these triangles. A switching vector comprising a number of switching states represents the vertices of each triangle. There are m^3 switching states for m -level inverter. The on-time equations of SVPWM execute the switching states of the triangle. The performance of the inverter significantly depends on the selection of these switching states [6]. Triangle numbers, switching states increase with the increase of level that creates computational complexity in terms of on-time calculations. There are a number of space vector algorithms that shows the better performance. Some of them some are mentioned with their limitations. Celanovic and Boroyevich presented a euclidean vector system based SVPWM algorithm that needs several matrix transformations, lacks of regular sequence of determining the switching states and is unsuitable for real-time implementation [7]. The method proposed by Loh and Holmes [8] with two level on-time calculation will result in total computations higher than Celanovic and Boroyevich [7]. Authors [9] introduce a method for on-time calculation that works well only up to three levels. The multilevel ON-time calculation problem is converted to a simple two-level ON-time calculation problem. J. H. Seo and C. H. Choi [10] proposed a technique for a three-level inverter based on two level inverter. The three-level space vector diagram is divided into six two-level space vector diagrams. A two-phase to three-phase conversion is needed to calculate the point to shift of origin of a virtual two-level inverter. Subsequent to the shift of origin and 60° coordinate transformation, on-times are calculated using two-level equations. Even for three levels, this technique requires more computations than the presented technique [6]. Trabelsi and Ben-Brahim [11] proposed a new space vector algorithm that needed separate equations to calculate on-times for odd and even number triangle determination.

In this paper, we presented a simple algorithm to perform the SVPWM for diode clamped three level inverter. The on-time calculation is based on two level SVPWM algorithm that is simple and the on-time calculation equations do not change with the position of reference vector like the conventional algorithm. In the space vector diagram of an m -level inverter, the triangle where the reference vector is located is identified as integer Δ_n . Any switching sequence can be executed with respect to triangle Δ_n , leading to an easiness and flexibility of optimizing the switching sequence. Three level space vector diagram is divided into six sector each containing four triangle shown in figure 1. Shantanu Chatterjee used 7 switching states for triangle 1, 4 switching states for triangle 2 and 4 and 5 switching states for triangle 3 that needed more memory space, more computation time and more lookup table [12]. In this control technique, there have been proposed only four active switching states in each triangle shown in Table 1 that required less number of lookup table and computations. This technique can be used for any m -level inverter without any significant increase in computations.

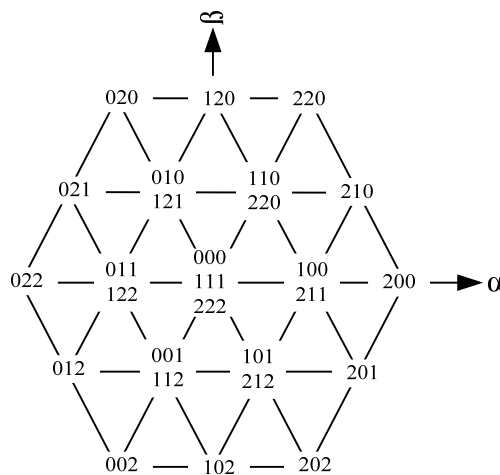


Figure 1. Space vector diagram for three level inverter

2. SVPWM ALGORITHM

Nupur Mittal and Bindeshwar Singh presented different PWM techniques applied for controlling the active devices in a multilevel inverter [13]. In this paper, SVPWM technique is presented to produce PWM control signals to the inverter. SVPWM compensates the required volt-seconds using discrete switching states and their on-times. The classical two-level space vector geometry can be used for on-time calculation. The space vector diagram of a three phase voltage source inverter is a hexagon, consisting of six sectors. Every sector is an equilateral triangle of unity side and $h (= \sqrt{3}/2)$ is the height of a sector. The on-time calculation is same for all sectors. Volt-second equation is:

$$V^z T_s = V_x T_a + V_y T_b \quad (1)$$

The volt-seconds in terms of components V^z , V_x and V_y of along $\alpha - \beta$ axis are,

$$V_\alpha^z T_s = T_a + \frac{1}{2} T_b \quad (2)$$

$$V_\beta^z T_s = h T_b \quad (3)$$

$$T_s = T_a + T_b + T_0 \quad (4)$$

Solving Equation (2)–(4), obtain for the calculation of ON times,

$$T_a = T_s \left[V_\alpha^z - \left(\frac{V_\beta^z T_s}{2h} \right) \right] \quad (5)$$

$$T_b = T_s \left[\frac{V_\beta^z}{h} \right] \quad (6)$$

$$T_0 = T_s - T_a - T_b \quad (7)$$

Where $T_s = 1/2f_s$, f_s is the switching frequency. For any given reference vector, the sector of operation and its angle within the sector is determined by using Equation (8) and (9), respectively.

$$S_i = \text{int} \left(\frac{\theta}{60} \right) + 1 \quad (8)$$

$$\gamma = \text{rem} \left(\frac{\theta}{60} \right) \quad (9)$$

In eqns. (8) and (9), $\theta (0 \leq \theta \leq 360)$ is the angle of the reference vector with respect to x-axis, $\gamma (0 \leq \gamma \leq 60)$ is the angle within the sector and $S_i (1 \leq S_i \leq 6)$ is its sector operation, int and rem are standard math function of integer and remainder.

In each sector, triangle can be classified into two types. Type 1 triangle has its base side at the bottom. Type 2 triangle has its base side at the top. The triangle number Δ_n can be determined in terms of two integer variables P_1 and P_2 , which are dependent on the position of reference vector (V_α , V_β).

$$P_1 = \text{int} \left(V_\alpha + \frac{V_\beta}{\sqrt{3}} \right) \quad (10)$$

$$P_2 = \text{int} \left(\frac{V_\beta}{h} \right) \quad (11)$$

P_1 represents the part of the sector between the two lines joining the vertices, separated by distance h and inclined at 120° with respect to α -axis shown in Figure 2. $P_1 = 0$ signifies that the point Q is below line A_1A_2 . $P_1 = 1$ signifies that the point Q is between line A_1A_2 and line A_3A_5 . P_2 represents the part of the sector between the two lines joining the vertices, separated by distance h and parallel to α -axis. $P_2 = 0$ signifies that the point Q is between line A_0A_3 and line A_2A_4 . $P_2 = 1$ signifies that the point Q is above line A_2A_4 . Geometrically, the values of P_1 and P_2 are an intersection of two rectangular regions which is either a triangle or rhombus. In other words, the point Q lies in (a) triangle Δ_0 if $P_1 = 0$ and $P_2 = 0$, (b) rhombus $A_1A_3A_4A_2$ if $P_1 = 1$ and $P_2 = 0$, (c) triangle Δ_3 if $P_1 = 1$ and $P_2 = 1$. The same analogy can be used for any level. In Figure 2, the reference vector is located in rhombus $A_1A_3A_4A_2$. This rhombus is made up of two

triangles Δ_1 and Δ_2 . The point Q can be located in any of the two. Let $(V_{\alpha i}, V_{\beta i})$ be the coordinates of the point Q with respect to the point A_1 obtained as:

$$V_{\alpha i} = V_{\alpha} - P_1 + .5P_2 \quad (12)$$

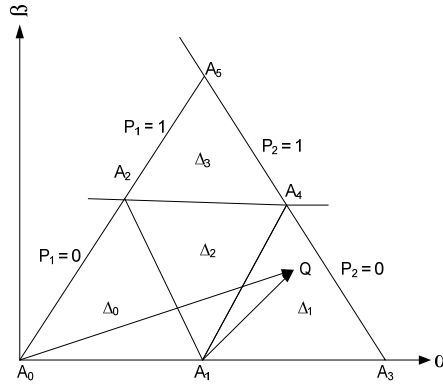


Figure 2. Space vector diagram of triangle determination for sector 1

$$V_{\beta i} = V_{\beta} - P_2 h \quad (13)$$

In Equation (12) and (13), $(V_{\alpha i}/V_{\beta i})$ is the slope of the line between the origin of the rhombus and the reference vector and it is compared with slope of the diagonal of the rhombus which is $\sqrt{3}$.

The slope comparison is done by evaluating inequality $(V_{\beta i} \leq \sqrt{3}V_{\alpha i})$ and to determine the small vector V^z and the exact triangle number Δ_n . If $(V_{\beta i} \leq \sqrt{3}V_{\alpha i})$ which indicates triangle of type 1 and these triangles are similar to sector 1 of two-level inverter. The triangle number Δ_n is obtained as:

$$\Delta_n = P_1^2 + 2P_2 \quad (14)$$

If $(V_{\beta i} > \sqrt{3}V_{\alpha i})$ which indicates triangle of type 2 and these triangles are similar to sector 2 of two-level inverter. The triangle number Δ_n is obtained as:

$$\Delta_n = P_1^2 + 2P_2 + 1 \quad (15)$$

In Equation (14) and (15), Δ indicates the triangle and n is the triangle number and hence Δ_n is an integer and signifies nth triangle in the sector. Using eqns. (14) and (15), to identify triangle in a sector and the on times are calculated using Equation (5)–(7). The Δ_n is formulated to provide a simple way of arranging the triangle, leading to ease of identification and extension to any level.

3. CONTROL TECHNIQUE AND TOPOLOGY

The multilevel inverter is best suited for the application which demands the finest quality of the ac supply waveforms. This work presented a SVPWM control technique, which pertains full H-Bridge diode clamped multilevel inverters. Some researcher used $(m+1)$ number dc sources [4], [15] for developing their proposed model that increase the cost as well as make the system bulky. In this model, we used $(m-1)/2$ number of dc sources that are cost effective. The general function of this multilevel inverter is to synthesize a desired voltage from a single dc source which may be obtained from battery, fuel cell, or solar cell. Unlike the cascaded inverter, the diode clamp inverter does not require separate voltage sources for each half bridge. A three phase three-level full H-bridge inverter is shown in Figure 3. An m-level three phase full H-bridge inverter typically consists of $6(m-1)$ main switching devices and $6(m-2)$ main diodes. A three phase RL load of 50 ohm and 20 mH is connected across the output of inverter. The switching sequences for three phase three level inverter are given in Table 2 [16].

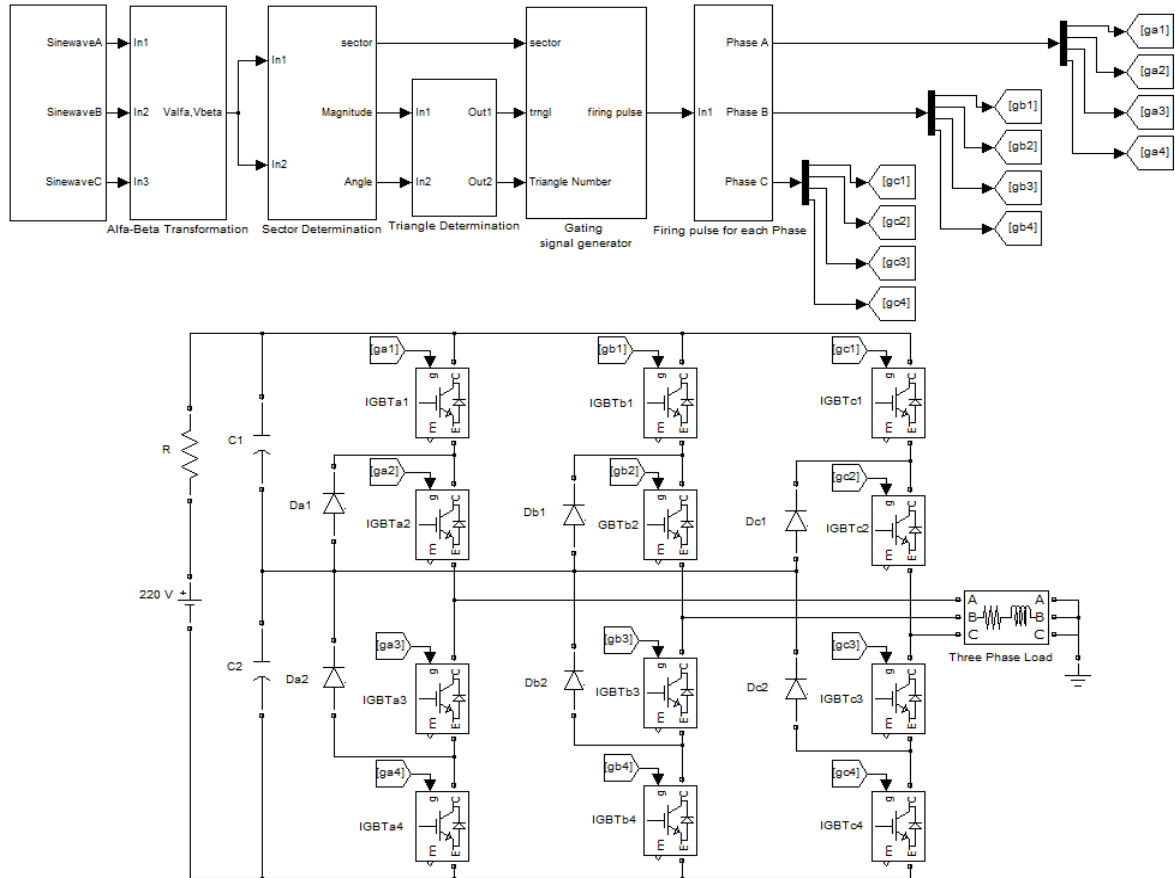


Figure 3. Complete simulation block diagram for the whole system

4. RESULT AND DISCUSSION

Simulations are performed for this system and compared with SPWM to validate the results by using MATLAB/Simulink and Origin 6.1. Three level inverter based on SVPWM is presented as 3LSVPWM and another is the same like this. Measurement of output currents are shown in Figure 4(a) and 4(b) for 2LSVPWM and 3LSVPWM respectively. Comparison of their harmonic distortion (HD) is shown in Figure 4(c). Fundamental harmonic distortion is always 100% that has been skipped due to simplicity of graphical presentation. The measurement of current THD for 2LSVPWM is 3.86% and for 3LSVPWM is 2.83%. The reduced current THD is found for 3LSVPWM by 1.03% than 2LSVPWM. Measurement of output currents are shown in Figure 4(d) and 4(e) for 2LSPWM and 3LSPWM respectively. Comparison of their HD is shown in Figure 4(f). The measurement of current THD for 2LSPWM is 10.69% and for 3LSPWM is 4.49%. 3LSPWM shows reduced THD than 2LSPWM by 6.2%. Comparison of Current HD between 3LSPWM and 3LSVPWM is shown in Figure 4(g). 3LSVPWM shows the reduction of THD than 3LSPWM by 1.66% that is the lowest current THD than any others. Measurement of output voltages are shown in Figure 4(h) and 4(i) for 2LSVPWM and 3LSVPWM respectively. Comparison of their HD is shown in Figure 4(j). The measurement of voltage THDs are 52.24% and 23.21% for 2LSVPWM and 3LSVPWM respectively. 29.03% reduced THD is found for 3LSVPWM than 2LSVPWM. Measurement of output voltages are shown in Figure 4(k) and 4(l) for 2LSPWM and 3LSPWM respectively. Comparison of their HD is shown in Figure 4(m). The measurement of voltage THDs are 64.67% and 36.63% for 2LSPWM and 3LSPWM respectively. 3LSPWM shows 28.04% reduced THD than 2LSPWM. Comparison of voltage HD between 3LSPWM and 3LSVPWM is shown in Figure 4(n). 3LSVPWM provides 13.42% reduced THD than 3LSPWM. Hence, 3LSVPWM shows the best performance than any others.

Table 1. Switching Sequence of Active Vectors for Three Level Inverter

Sector	Triangle No.	Sequence of Active Vectors
1	0	111-211-221-222
	1	100-200-210-211
	2	100-110-210-211
	3	110-210-220-221
2	0	111-121-221-222
	1	110-120-220-221
	2	110-120-121-221
	3	010-020-120-121
3	0	111-121-122-222
	1	010-020-021-121
	2	010-011-021-121
	3	011-021-022-122
4	0	111-112-122-222
	1	011-012-022-122
	2	011-012-112-122
	3	001-002-012-112
5	0	111-112-212-222
	1	001-002-102-112
	2	001-101-102-112
	3	101-102-202-212
6	0	111-211-212-222
	1	101-201-202-212
	2	101-201-211-212
	3	100-200-201-211

Table 2. Switching Sequence for Phase A

Switching Symbol	Switching States for Phase A				Terminal Voltage
	S _{a1}	S _{a2}	S _{a3}	S _{a4}	
P	1	1	0	0	V _{dc/2}
O	0	1	1	0	0
N	0	0	1	1	-V _{dc/2}

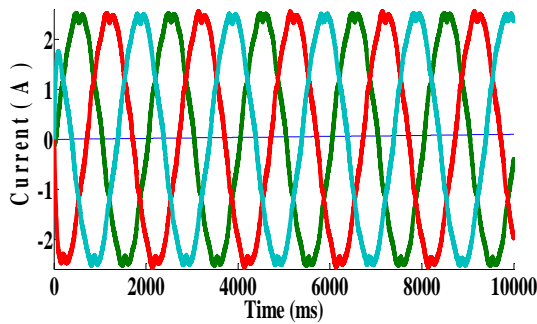


Figure 4(a). Output current for two level SVPWM

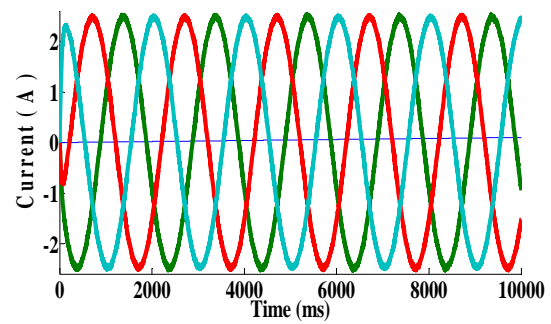


Figure 4(b). Output current for three level SVPWM

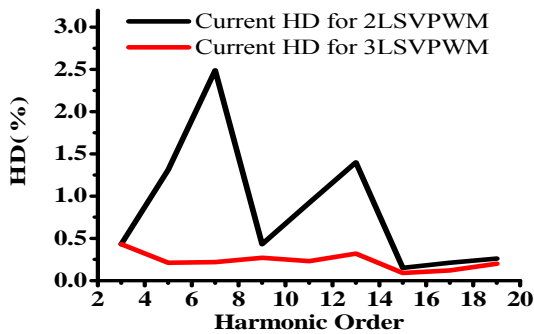


Figure 4(c). Comparison of Current HD between 2LSVPWM and 3LSVPWM

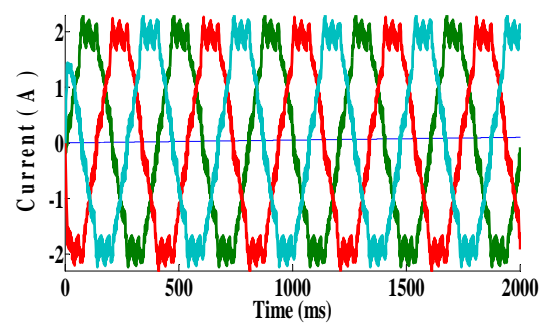


Figure 4(d). Output current for two level SPWM

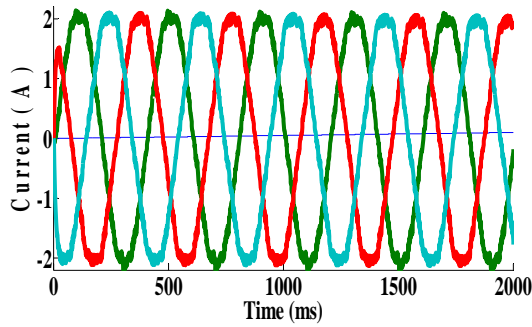


Figure 4(e) Output current for three level SPWM

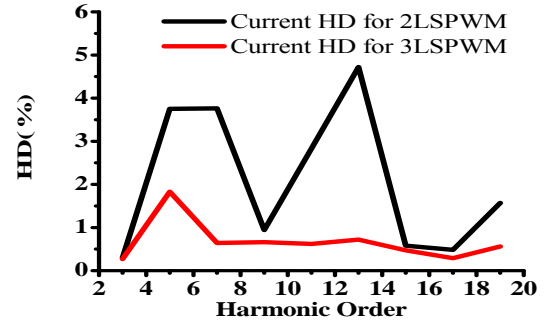


Figure 4(f). Comparison of Current HD between 2LSPWM and 3LSPWM

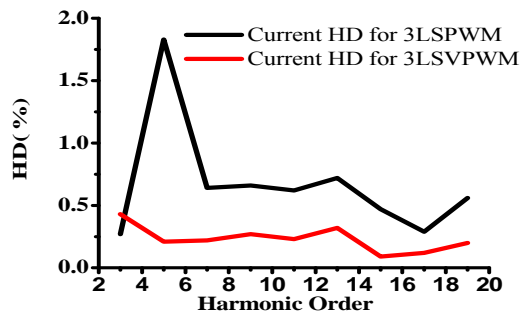


Figure 4(g). Comparison of Current HD between 3LSPWM and 3LSVPWM

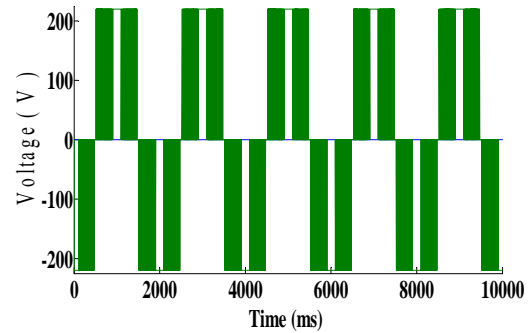


Figure 4(h). Output Voltage for two level SVPWM

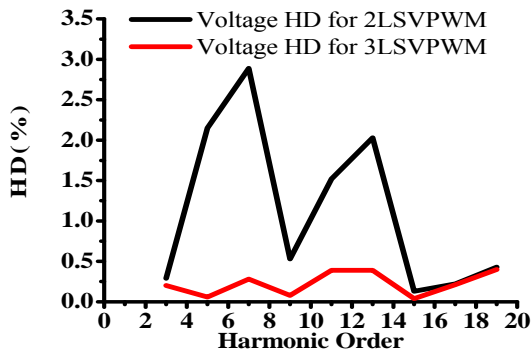


Figure 4(i). Output Voltage for three level SVPWM

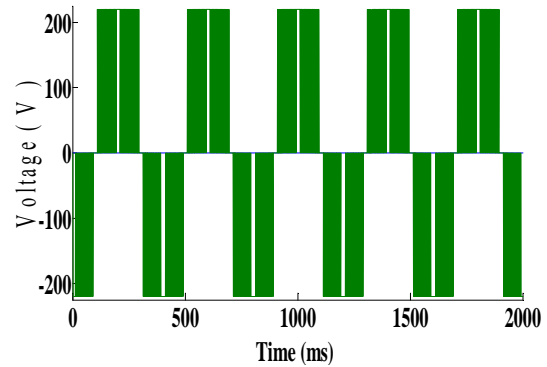


Figure 4(j). Comparison of Voltage HD between 2LSVPWM and 3LSVPWM

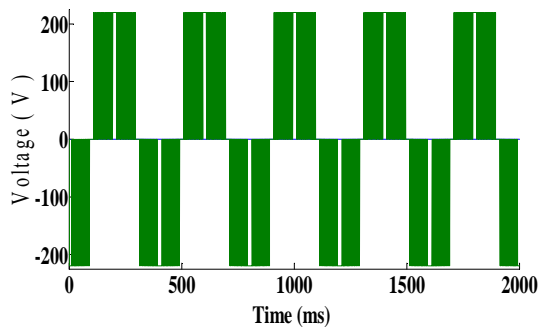


Figure 4(k). Output Voltage for two level SPWM

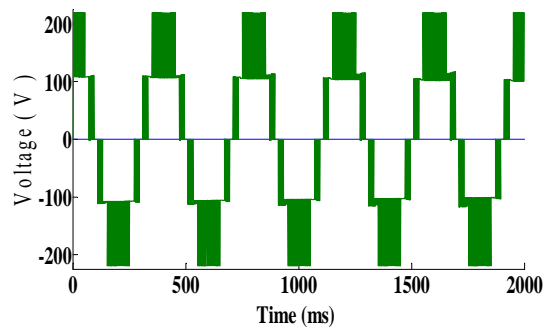


Figure 4(l). Output Voltage for three level SPWM

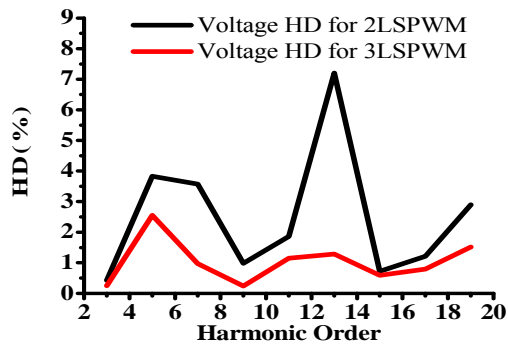


Figure 4(m). Comparison of Voltage HD between 2LSPWM and 3LSPWM

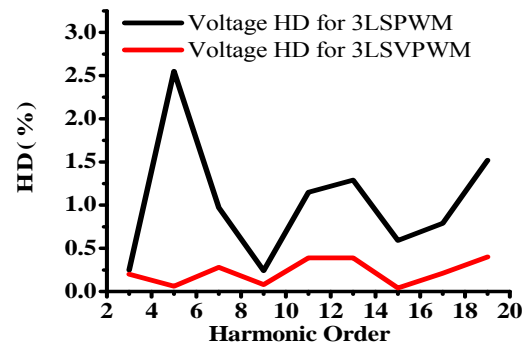


Figure 4(n). Comparison of Voltage HD between 3LSPWM and 3LSVPWM

5. CONCLUSION

This paper represents diode clamped three level inverter based on space vector pulse width modulation and analyzed in details. Simulations are performed with reduced number of switching states (four active switching states) this system and compared with SPWM to validate the results by using MATLAB/Simulink and Origin 6.1. From the simulation results, 2LSVPWM shows better performance than 2LSPWM. Furthermore, 3LSVPWM shows better performance than both 2LSVPWM and 3LSPWM in terms of THD. Hence, it can be concluded that 3LSVPWM gives enhanced fundamental output with better quality i.e. lesser THD compared to the others.

ACKNOWLEDGEMENTS

This work has been supported by Malaysian Technical Universities Network (MTUN) grant. We would like to thank all the research students of the Research Laboratory of Electric Vehicle and Drive in UTeM for their help in solving many critical problems.

REFERENCES

- [1] Jose Rodriguez, Steffen Bernet, Peter K Steimer, Ignacio E Lizama. A Survey on Neutral-Point-Clamped Inverters. *IEEE Transactions on Industrial Electronics*. 2010; 57(7).
- [2] José Rodríguez, Jih-Sheng Lai, Fang Zheng Peng. Multilevel Inverters: A Survey of Topologies, Controls, and Applications. *IEEE Transactions on Industrial Electronics*. 2002; 49(4).
- [3] Colak, İlhami, Kabalcı, Ersan, Bayindir, Ramazan. Review of multilevel voltage source inverter topologies and control schemes. *Energy Conversion and Management*. 2011; 52(2): 795-1574.
- [4] Amit Kumar Gupta, Ashwin M Khambadkone. A General Space Vector PWM Algorithm for Multilevel Inverters, Including Operation in Overmodulation Range. *IEEE International Conference on Electric Machines and Drives*. 2005: 1437-1444.
- [5] Saravanan M, Nandakumar R, Veerabalaaji G. Effectual SVPWM Techniques and Implementation of FPGA Based Induction Motor Drive. *International Journal of Reconfigurable and Embedded Systems*. 2012; 1(1): 11-18.
- [6] Amit Kumar Gupta, Ashwin M Khambadkone. A Space Vector PWM Scheme for Multilevel Inverters Based on Two-Level Space Vector PWM. *IEEE Transactions on Industrial Electronics*. 2006; 53(5).
- [7] Nikola Celanovic, Dushan Boroyevich. A Fast Space-Vector Modulation Algorithm for Multilevel Three-Phase Converters. *IEEE Transactions on Industry Applications*. 2001; 37(2).
- [8] Poh Chiang Loh, Donald Grahame Holmes. Flux Modulation for Multilevel Inverters. *IEEE Transactions on Industry Applications*. 2002; 38(5).
- [9] Haoran Zhang, Annette von Jouanne, Shaoan Dai. Multilevel Inverter Modulation Schemes to Eliminate Common-Mode Voltages. *IEEE Transactions on Industry Applications*. 2000; 36(6).
- [10] JH Seo, CH Choi, DS Hyun. A new simplified space-vector pwm method for three-level inverters. *IEEE Trans. Power Electron*. 2001; 16(4): 545-550.
- [11] M Trabelsi, L Ben-Brahim, T Yokoyama, A Kawamura, R Kurosawa, T Yoshino. An Improved SVPWM Method for Multilevel Inverters. *15th International Power Electronics and Motion Control Conference*. 2012: LS5c.1-1 - LS5c.1-7.
- [12] Shantanu Chatterjee. A Multilevel Inverter Based on SVPWM Technique for Photovoltaic Application. *International Journal of Power Electronics and Drive System*. 2013; 3(1): 62-73.

- [13] Nupur Mittal, Bindeshwar Singh, SP Singh, Rahul Dixit, Dasharath Kumar. Multilevel Inverters: A Literature Survey on Topologies and Control Strategies. *2nd International Conference on Power, Control and Embedded Systems*. 2012: 1 – 11.
- [14] M ValanRajkumar, PS Manoharan. FPGA based multilevel cascaded inverters with SVPWM algorithm for photovoltaic system. *Solar Energy*. 2013; 87: 229–245.
- [15] Amit Kumar Gupta, Ashwin M Khambadkone. A General Space Vector PWM Algorithm for Multilevel Inverters, Including Operation in Overmodulation Range. *IEEE Transactions on Power Electronics*. 2007; 22(2).
- [16] Lin Lei, ZhongHeqing, Deng Yu, Zhang Jie, ZouYunping, She Xu. A DTC Algorithm for Three-level Induction Motor Drives System Based on Discrete Space Vector Modulation. *Twenty-Fourth Annual IEEE Applied Power Electronics Conference and Exposition*. 2009: 1978-1983.